Parasitology Research (2018) 117:265–271
https://doi.org/10.1007/s00436-017-5701-x

ORIGINAL PAPER

Silver nanoparticle conjugation affects antiacanthamoebic activities of amphotericin B, nystatin, and fluconazole

Ayaz Anwar[1] · Ruqaiyyah Siddiqui[1] · Muhammad Asim Hussain[2] · Dania Ahmed[2] · Muhammad Raza Shah[2] · Naveed Ahmed Khan[1]

Received: 14 September 2017 / Accepted: 27 November 2017 / Published online: 7 December 2017

Abstract

Infectious diseases are the leading cause of morbidity and mortality, killing more than 15 million people worldwide. This is despite our advances in antimicrobial chemotherapy and supportive care. Nanoparticles offer a promising technology to enhance drug efficacy and formation of effective vehicles for drug delivery. Here, we conjugated amphotericin B, nystatin (macrocyclic polyenes), and fluconazole (azole) with silver nanoparticles. Silver-conjugated drugs were synthesized successfully and characterized by ultraviolet-visible spectrophotometry, Fourier transform infrared spectroscopy, and atomic force microscopy. Conjugated and unconjugated drugs were tested against *Acanthamoeba castellanii* belonging to the T4 genotype using amoebicidal assay and host cell cytotoxicity assay. Viability assays revealed that silver nanoparticles conjugated with amphotericin B (Amp-AgNPs) and nystatin (Nys-AgNPs) exhibited significant antiamoebic properties compared with drugs alone or AgNPs alone ($P < 0.05$) as determined by Trypan blue exclusion assay. In contrast, conjugation of fluconazole with AgNPs had limited effect on its antiamoebic properties. Notably, AgNP-coated drugs inhibited amoebae-mediated host cell cytotoxicity as determined by measuring lactate dehydrogenase release. Overall, here we present the development of a new formulation of more effective antiamoebic agents based on AgNPs coated with drugs that hold promise for future applications.

Keywords *Acanthamoeba* · Silver nanoparticles · Amphotericin B · Nystatin · Fluconazole

Introduction

Acanthamoeba is a protist that is widely distributed in the environment (Marciano-Cabral and Cabral 2003; Visvesvara et al. 2007). Based on rDNA sequencing, *Acanthamoeba* has been divided into 21 different genotypes, named T1 to T21 (Fuerst et al. 2015). *Acanthamoeba* consists of both pathogenic and non-pathogenic isolates. Given the opportunity and access, pathogenic *Acanthamoeba* can produce serious infections involving the central nervous system, known as granulomatous amoebic encephalitis (GAE) as well as sight-threatening infection, known as *Acanthamoeba* keratitis (Martinez and Visvesvara 1991). Treatment involves application of a mixture of drugs including biguanide compounds, amidine derivatives, and azole compounds that can last for months with toxic effects on host cells/tissues (Seal et al. 1995; Ishibashi et al. 1990; Visvesvara et al. 2007). This is despite our advances in antimicrobial chemotherapy and supportive care. Due to challenges in the discovery of novel drugs and/or approvals by regulatory authorities for clinical use, repurposing of clinically approved drugs is a useful avenue of research (O'Connell et al. 2013). This approach is particularly attractive against neglected diseases where there is limited interest by the pharmaceutical industry.

Targeting ergosterol biosynthesis is a major pathway for drug development against fungal infections. Since ergosterol is also present in the plasma membrane of *Acanthamoeba*, it is proved to be a rational drug target against *Acanthamoeba* infections. However, several ergosterol pathway-targeting drugs show limited clinical value due to host cell cytotoxicity when used against *Acanthamoeba* infections at higher doses (Girois et al. 2006; Martín-Navarro et al. 2015; Thomson et al.

✉ Naveed Ahmed Khan
naveed5438@gmail.com

[1] Department of Biological Sciences, School of Science and Technology, Sunway University, 47500 Subang Jaya, Selangor, Malaysia

[2] International Center for Chemical and Biological Sciences, H.E.J. Research Institute of Chemistry, University of Karachi, Karachi 75270, Pakistan

2017). Since ergosterol is also present in the plasma membrane of *Acanthamoeba*, it is proved to be a rational drug target for drugs against *Acanthamoeba* infections. Metal nanoparticles have a high surface area and therefore have ability to display unique physicochemical characteristics and biological activities especially against infectious diseases (Zazo et al. 2016). It is well known that silver-based compounds are capable of exhibiting strong biocidal efficacy on numerous bacteria and parasites (Zhao and Stevens 1998; Li et al. 2014; Yang et al. 2017). The formation of nanoparticles enhances bioavailability and efficacy of drugs (Maincent et al. 1986). Nanoparticles have been successfully utilized in the enhancement of bioactivity of drugs (Grace and Pandian 2007; Aqeel et al. 2016), as well as for improvement of administration routes for drug delivery such as systemic, oral, pulmonary, and transdermal routes (Wilczewska et al. 2012). As the *Acanthamoeba* plasma membrane contains ergosterol as an important constituent, here we tested whether conjugation of silver nanoparticles (AgNPs) can enhance efficacy, at reduced concentration, of fluconazole (mode of action involves inhibition of cytochrome P450 enzyme 14α-demethylase to prevent conversion of lanosterol to ergosterol), amphotericin B (mode of action involves binding to ergosterol leading to formation of pores), and nystatin (targeting ergosterol to form pores in the plasma membrane). Silver nanoparticle-conjugated drugs were synthesized by one phase reduction of silver nitrate via sodium borohydride in the presence of drugs. The synthesized nanoparticles were characterized by ultraviolet-visible (UV-Vis) spectrophotometry, fourier-transform infrared (FT-IR) spectroscopic analysis, and size determination by Atomic Force Microscope (AFM). Drug-conjugated AgNPs were tested for amoebicidal properties against *A. castellanii* clinical isolate belonging to the T4 genotype.

Materials and methods

Chemicals

All chemicals used in the synthesis of drug-conjugated AgNPs were of analytical grade. Silver nitrate and sodium borohydride were purchased from Merck chemicals, while amphotericin B, nystatin, fluconazole, and all other chemicals were purchased from Sigma-Aldrich unless otherwise stated.

Synthesis of drug-coated AgNPs

Synthesis of amphotericin B-, nystatin-, and fluconazole-coated AgNPs was achieved by simple reduction of silver nitrate aqueous solution with sodium borohydride in the presence of drugs as described previously (Anwar et al. 2016). Briefly, 5 mL (0.1 mM) of amphotericin B aqueous solution was reacted with 5 mL (0.1 mM) silver nitrate aqueous solution, and the reaction mixture was magnetically stirred for 10 min. Next, 30 μL of 4 mM freshly prepared sodium borohydride aqueous solution was added in the above stirring reaction mixture. The color of solution turned yellow-brown from transparent on addition of reducing agent indicating the reduction of silver ions and formation of Amp-AgNPs. For Nys-AgNPs and Flu-AgNPs, a similar procedure was repeated by optimizing different *v*/*v* ratios of silver solution and drugs. Stable Nys-AgNPs and Flu-AgNPs were obtained at a respective volume ratio of silver to drug at 4:1 and 1:1. Unprotected bare AgNPs were also obtained by the same procedure in the absence of any drug or stabilizing agent, but were freshly prepared when required due to their kinetic unstability which results into aggregation. All synthesized nanoparticles were centrifuged at 10000×*g* for 20 min to separate large aggregates, excess unbound ligand, and side products from colloidal suspension followed by redispersion in deionized water. These synthesized nanoparticles were subjected to characterization by UV-Vis spectrophotometer (Evolution 300, Thermo Scientific) and FT-IR spectroscope (Vector 22, Bruker), while morphological analysis was carried out using AFM (Agilent 5500) as described previously (Anwar et al. 2016).

Henrietta lacks cervical adenocarcinoma cells (HeLa) cells culture

HeLa cells were routinely cultured in a 75-cm^2 culture flask in RPMI-1640 containing 10% FBS, 10% Nu-serum, 2 mM glutamine, 1 mM pyruvate, penicillin (100 units/mL), streptomycin (100 μg/mL), non-essential amino acids, and vitamins. The confluent flasks were trypsinized after removal of old media with 2 mL trypsin, followed by centrifugation for 5 min at 2000×*g*. Cell pellet was resuspended in 30 mL media, and 200 μL of cell suspension was seeded in each well of a 96-well plate. The plate was then incubated at 37 °C in a 5% CO_2 incubator with 95% humidity for 24 h. The plates were observed under light microscope for the formation of uniform monolayer of HeLa cells, and used for cytotoxicity assay.

Acanthamoeba cultures

A. castellanii (ATCC 50492), a clinical isolate belonging to the T4 genotype, was cultured in 10 mL proteose peptone 0.75% (*w*/*v*), yeast extract 0.75% (*w*/*v*), and glucose 1.5% (*w*/*v*) (PYG) medium at 30 °C in 75-cm^2 tissue culture flasks as reported previously (Sissons et al. 2006). For amoebicidal assays, active trophozoites were used which are adherent to the surface of flasks. *A. castellanii* trophozoites were obtained by changing PYG media with 10 mL RPMI-1640, and the culture flask was left on ice for 15 min and gently tapped for 5 min (Sissons et al. 2006). Finally, *A. castellanii* suspension was transferred to a 50-mL tube, followed by centrifugation at 2500×*g* for 10 min. Amoeba pellet was resuspended in 1 mL RPMI-1640, counted using a hemocytometer, and used for amoebicidal assay.

Amoebicidal assay

The amoebicidal potential of drugs alone, drugs conjugated with AgNPs, and AgNPs alone were determined as previously described (Sissons et al. 2006). Briefly, 5×10^5 *A. castellanii* per well were incubated with 5 and 10 μM concentrations of drugs or relevant amounts of solvent/AgNPs alone in RPMI-1640 in 24-well plates. RPMI-1640 alone was used as a negative control while 30 μM chlorhexidine was used as a positive control for this assay. Plates were incubated at 30 °C for 24 h. The viability of amoebae was determined by adding 0.1% Trypan blue to each well and counting live (non-stained) *A. castellanii* using a hemocytometer. The data are represented as the mean ± standard error of at least three independent experiments performed in duplicate.

Acanthamoeba-mediated host cell cytotoxicity assay

Amoebae-mediated HeLa cell cytotoxicity was evaluated as described previously (Khan and Siddiqui 2009; Ali et al. 2017). Briefly, assays were performed in 96-well plates containing confluent HeLa monolayers. Amoebae (8×10^4) treated with various drugs conjugated with AgNPs, AgNPs alone, and drugs alone (5 and 10 μM concentration) followed by 2 h incubation at 30 °C. Additionally, untreated amoeba and amoeba treated with chlorhexidine were also used as controls. After incubation, these samples and controls were centrifuged at 5000×*g* for 1 min to remove the extracellular materials and the pellet was resuspended in 200 μL fresh RPMI followed by addition to HeLa cells. Plates were incubated at 37 °C in a 5% CO_2 incubator for 24 h. Negative control values for cytotoxicity assays were obtained by incubating HeLa cells with RPMI-1640 alone, and positive control values were obtained by 100% cell death using 1% Triton X-100. After incubation, supernatants were collected from each well and lactate dehydrogenase (LDH) release was measured using cytotoxicity detection assay kit as described previously (Aqeel et al. 2016). The LDH is an intracellular enzyme, and it is only released from damaged cells. The percent cytotoxicity was calculated as follows: % cytotoxicity = (sample absorbance − negative control absorbance) / (positive control absorbance − negative control absorbance) × 100.

Results

Characterization of drugs conjugated with AgNPs using UV-Vis, FT-IR spectroscopy, and AFM

Synthesized AgNP-conjugated drugs were subjected to UV-Vis spectrophotometry, FT-IR spectroscopy, and AFM analysis for confirmation of synthesis and determination of size and stability. Amp-AgNPs, Nys-AgNPs, and Flu-AgNPs were successfully synthesized by protocols mentioned above. UV-Vis spectra of Amp-AgNPs gave maximum absorption at 424 nm (Fig. 1) as compared to pure amphotericin B which gives multiple absorption bands in the range of 280–400 nm (Radwan et al. 2017) which implies its stabilizing interaction with AgNPs. Nys-AgNPs and Flu-AgNPs showed a characteristic surface plasmon resonance (SPR) band for AgNPs at 405 and 400 nm, as compared to bands around 280–330 and 260 nm, respectively, for pure nystatin and fluconazole (Rodino et al. 2014; Singh et al. 2011). For size and morphological determination, AFM images were recorded. All nanoparticle samples were found to be spherical in shape and polydispersed in size. Drug-conjugated AgNPs were in the wide size range of 10–90 nm as borohydride reduction method is a rapid but unselective with respect to size distribution. Figure 2 shows representative AFM topographic images of Nys-AgNPs and Flu-AgNPs.

FT-IR spectral analysis of fluconazole and Flu-AgNPs shows chemical modifications involved in the stabilization of AgNPs with drug molecules. The FT-IR spectrum of fluconazole alone is compared with the Flu-AgNPs to elucidate stabilizing functionalities in drugs as a representative example as shown in Fig. 3. Fluconazole alone showed an absorption band at 3116 for CH stretching, 1620 for fluorinated benzyl group, 1413 for triazole ring stretching, 1272 for OH stretching, 1080 for COH stretching, and 966 for OCH stretching vibrations which are also supported by earlier work of Bourichi et al. (2012). After the formation of Flu-AgNPs, the major changes which appeared were 3116 CH stretching vibration and triazole stretching vibration shifted to 3406 and 1390, respectively, while 1510 triazole C=C stretching vibration disappeared. Stretching vibrations appeared at 1080 for C-H, and at 966 for O-CH triazole ring, vibration disappeared. These results clearly indicate the involvement of triazole ring and OH functionality present at the propane backbone in the fluconazole molecule in the stabilization of AgNPs.

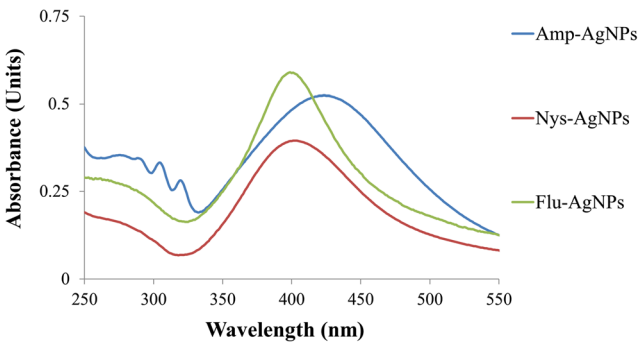

Fig. 1 UV-Vis spectra of drug-coated AgNPs showed surface plasmon resonance bands at 424, 405, and 400 nm for Amp-AgNPs, Nys-AgNPs, and Flu-AgNPs, respectively, which indicates the successful formation of drug-conjugated AgNPs

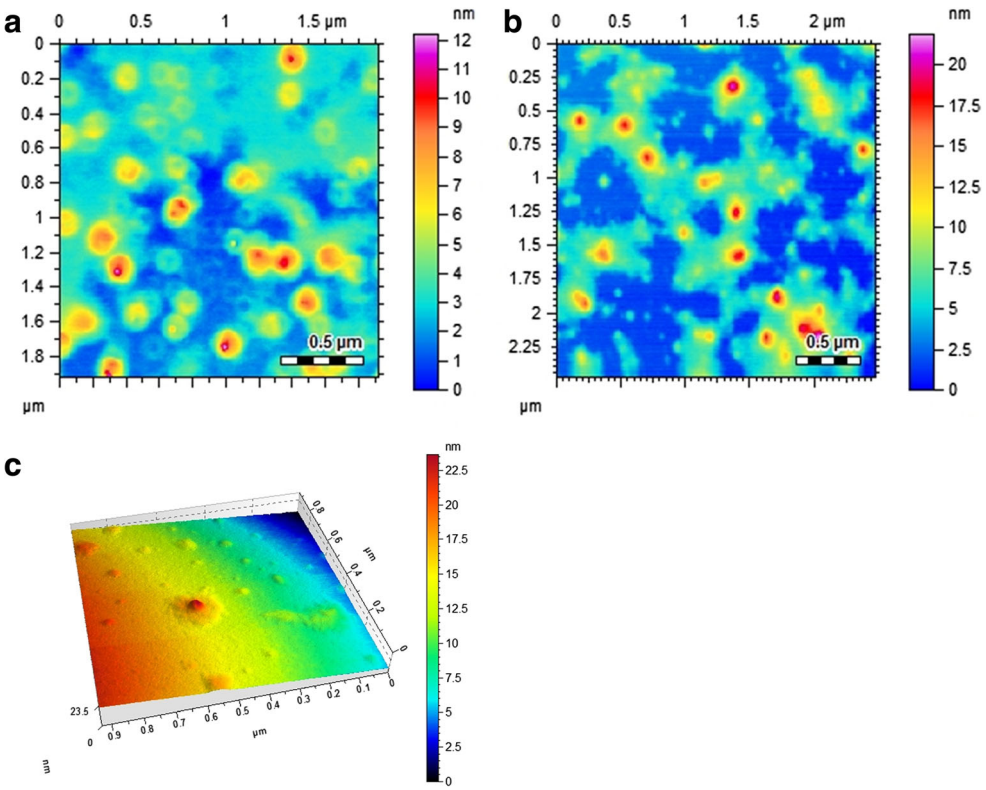

Fig. 2 AFM topographic images of Nys-AgNPs (**a**), Flu-AgNPs (**b**), and bare AgNPs (**c**) show the size and morphology of synthesized nanoparticles. All synthesized materials are found to be spherical and polydispersed in size distribution ranging in size domain of 10 to 90 nm. For AFM analysis, samples were loaded on mica surface and air dried followed by tapping mode image recording with a silicon nitride cantilever using an Agilent 5500 atomic force microscope. The results describe representative images of several experiments

Drugs conjugated with AgNPs exhibited increased amoebicidal effects against *A. castellanii* compared with drugs alone

Amoebicidal assays were performed to determine the effects of drugs conjugated with AgNPs and drugs alone on the viability of *A. castellanii*. The results revealed that drugs conjugated with AgNPs exhibited significant amoebicidal effects against *A. castellanii* ($P < 0.05$ using two-sample T test and two-tailed distribution) (Fig. 4). Conversely, treatment with bare AgNPs alone had no effects on amoebae viability. Notably, Amp-AgNPs and Nys-AgNPs showed significant amoebicidal effects at 10 μM compared with drugs alone ($P < 0.05$ using two-sample T test and two-tailed distribution) (Fig. 4). When incubated with drugs alone, at 5 μM of nystatin, amoeba numbers were reduced to 1.5×10^5 (from 5×10^5). However, 5 μM Nys-AgNPs reduced amoeba numbers to 5×10^4 ($P < 0.05$ using two-sample T test and two-tailed

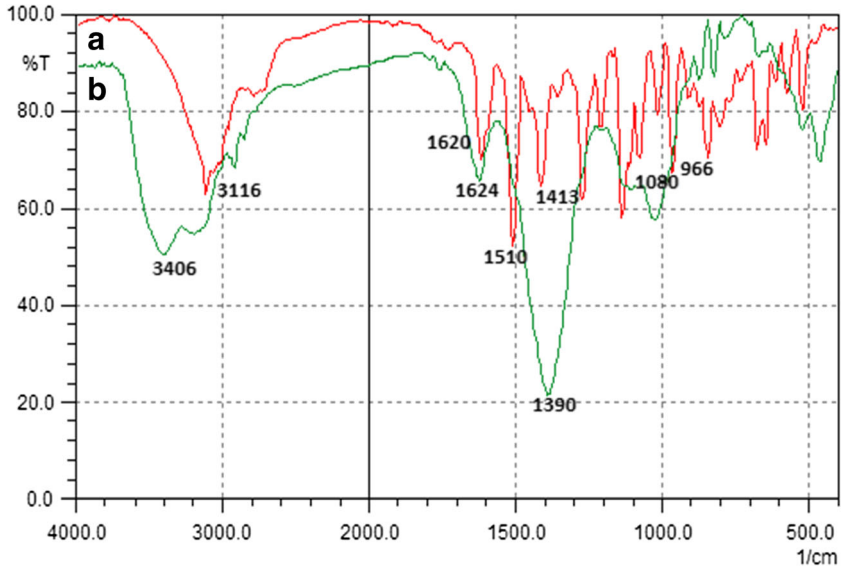

Fig. 3 Comparative FT-IR spectra of Flu-AgNPs (**a**) and fluconazole alone (**b**). Results showed that triazole ring and the OH group of fluconazole are conjugated with AgNPs and are responsible for the stabilization of AgNPs. FT-IR spectra were obtained by KBr disc method using Bruker Vector 22 FT-IR spectrometer. The results are representative of several experiments

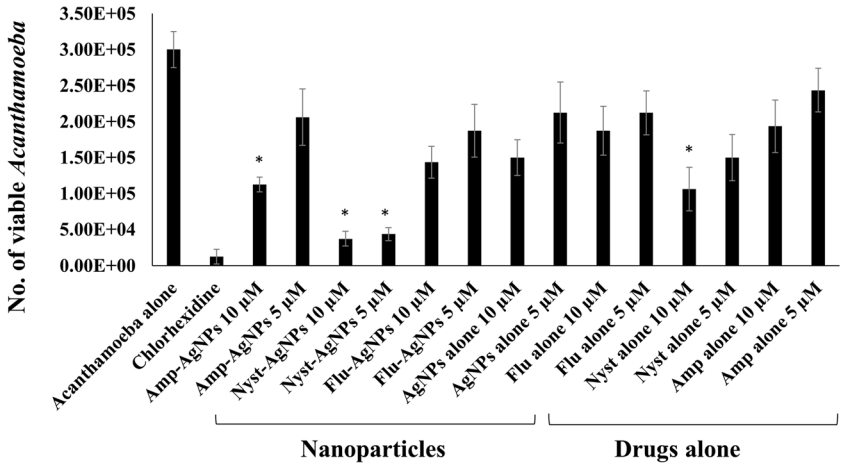

Fig. 4 *A. castellanii* viability was determined following incubation with various drugs as described in the "Materials and methods" section. Briefly, 5×10^5 *A. castellanii* were incubated with drugs and controls at 30 °C for 24 h. Next, amoebae viability was determined using Trypan blue exclusion assay. All three drug-conjugated AgNPs and drugs alone exhibited amoebicidal effects. Notably, Amp-AgNPs and Nys-AgNPs showed significant amoebicidal effects at 10 μM compared with drugs alone ($P < 0.05$ using two-sample T test and two-tailed distribution). The results are presented as the mean ± standard error of at least three independent experiments performed in duplicate

distribution). Amphotericin B alone did not show significant amoebicidal effects at 5 or 10 μM, while, at 10 μM Amp-AgNPs only, amoeba numbers were significantly reduced to 1.13×10^5 (from 5×10^5) ($P < 0.05$ using two-sample T test and two-tailed distribution). In contrast, conjugation of fluconazole with AgNPs did not enhance amoebicidal effects (Fig. 4). In particular, Nys-AgNPs showed potent amoebicidal effects of more than 90% (Fig. 4).

Silver nanoparticle-conjugated drugs inhibited *A. castellanii*-mediated host cell cytotoxicity

To determine whether AgNP-conjugated drugs inhibit amoebae-mediated host cell cytotoxicity, assays were performed as described in the "Materials and methods" section. When incubated with host cells, *A. castellanii* alone produced 75% host cell cytotoxicity. On the other hand, amoebae pretreated with chlorhexidine as well as Nys-AgNPs and Amp-AgNPs caused minimal host cell damage and host cell cytotoxicity was reduced to 21 and 27%, respectively.

Discussion

Acanthamoeba infections have remained significant despite our advances in antimicrobial chemotherapy. The lack of development and approval of new and effective antimicrobials as well as growing multiple-drug resistance of microbes presents a major challenge in our ability to counter parasitic infections (Khan 2006). Current approaches for development of new drugs rely mostly on chemical modifications of already existing molecular scaffolds known to have limited specificity for targets and high side effects. The conventional therapeutic agents against amoebae infections includes chlorhexidine, amphotericin B, fluconazole, rifampicin, pentamidine, PHMB, azithromycin, and/or a mixture of these drugs. However, the intravenous drug delivery of these drugs to CNS faces some major hurdles including blood-brain barrier (BBB) penetration, host-cell cytotoxicity, and ability of amoeba to form cysts. Therefore, there is an urgent need to develop new drugs, formulations, and chemotherapeutic strategies which can effectively overcome these challenges. Nanotechnology offers great promise in the field of biomedicines, especially diagnosis and drug delivery. It offers opportunities for therapeutic agent delivery to specific cells and receptors. Nanomaterial-based drug delivery systems have in general the potential to improve pharmacokinetics and pharmacodynamics of the drugs (Walsh et al. 2012). Nanotechnology-based drug delivery carriers have been developed and found their way into clinical practice such as liposomes and nanoparticles (Anselmo and Mitragotri 2016). Among drug delivery systems, nanoparticles hold pivotal position due to common advantages including (i) increased bioavailability, (ii) decreased side effects, (iii) lower dosage, (iv) specific and controlled drug release, etc. The small size of nanoparticles provides them a greater surface area for maximum drug loading as well as high accessibility for specific targets. Recently, various drug-conjugated nanoparticles are being developed against infections caused by resistant microbes (Zazo et al. 2016). The most common metal carriers for nanoparticle-based drug delivery systems include gold, silver, and iron oxide due to their inertness and biocompatibility (Wilczewska et al. 2012). Here, we determined the effects of AgNP conjugation with amphotericin B, nystatin, and fluconazole against *A. castellanii*. Drugs conjugated with

AgNPs were synthesized successfully. All drug-coated AgNPs showed SPR bands in the range of 400–450 nm, characteristic of medium-sized ligand-stabilized AgNPs. A broad SPR band was observed for Amp-AgNPs as compared to nystatin- and fluconazole-conjugated AgNPs suggesting formation of large-sized polydispersed nanoparticles. Since sodium borohydride is a strong and rapid reducing agent, its use for the synthesis of nanoparticles provides unselective size distribution as observed in AFM images. FT-IR spectral analysis of drugs conjugated with AgNPs showed that hydroxyl, carboxylic acid, and triazole functionalities are responsible for coating of drugs on the AgNP surface as well as their stabilization. Amoebicidal assay results revealed that drug-coated AgNPs are more effective against *A. castellanii* as compared to drugs alone. Nys-AgNPs in particular showed remarkable antiamoebic effects at both 10 and 5 μM concentrations. We also used host cell cytotoxicity assay as a secondary screen to test antiacanthamoebic agents. *A. castellanii* produced 75% cytotoxicity to host cells, while drug-coated AgNP pretreatment with amoeba resulted in a significant decrease in host cell cytotoxicity. The enhanced effects of nanoparticle-conjugated drugs as compared to pure drugs are likely due to enhanced transport of drugs to *A. castellanii*, as these drugs' translocation to a specific target is likely to be hindered due to their amphipathic nature, large size, and poor bioavailability (Radwan et al. 2017). The exact mechanism of AgNPs' antimicrobial potential is not completely understood so far; however, their efficacy tends to alter with modification in size, shape, and surface properties. Their antimicrobial activity is generally associated with multiple factors including AgNP interaction with microbial cell wall, release of toxic ions, penetration inside the cells, ROS and free radical generation, DNA damage, etc. (Dakal et al. 2016). In conclusion, these findings clearly showed that silver nanoparticles conjugation enhanced antiamoebic effects of drugs likely due to their small size and high drug loading ability. Nys-AgNPs and Amp-AgNPs were found to be most effective against *A. castellanii* as compared with drugs alone. As there are limited available options in the management and treatment of infections caused by *A. castellanii*, it is hoped that metal nanoparticles can be used as potential drug carriers for existing drugs in the improved therapies in biological systems. In vivo studies and especially administration of these drug-coated AgNPs via different routes for assessing their maximum biological potential will be tested in future studies against *Acanthamoeba* infections.

Compliance with ethical standards

Conflict of interest The authors declare that they have no conflict of interest.

References

Ali SM, Siddiqui R, Ong SK, Shah MR, Anwar A, Heard PJ, Khan NA (2017) Identification and characterization of antibacterial compound (s) of cockroaches (*Periplaneta americana*). Appl Microbiol Biotechnol 101(1):253–286. https://doi.org/10.1007/s00253-016-7872-2

Anselmo A, Mitragotri S (2016) Nanoparticles in the clinic. Bioeng Transl Med 1:10–29

Anwar A, Shah MR, Muhammad SP, Afridi S, Ali K (2016) Thiopyridinium capped silver nanoparticle based supramolecular recognition of Cu (I) in real samples and T-lymphocytes. New J Chem 40(7):6480–6486. https://doi.org/10.1039/C5NJ03609G

Aqeel Y, Siddiqui R, Anwar A, Shah MR, Khan NA (2016) Gold nanoparticle conjugation enhances the antiacanthamoebic effects of chlorhexidine. Antimicrob Agents Chemother 60(3):1283–1288. https://doi.org/10.1128/AAC.01123-15

Bourichi H, Brik Y, Hubert P, Cherrah Y, Bouklouze A (2012) Solid-state characterization and impurities determination of fluconazol generic products marketed in Morocco. J Pharm Anal 2(6):412–421. https://doi.org/10.1016/j.jpha.2012.05.007

Dakal TC, Kumar A, Majumdar RS, Yadav V (2016) Mechanistic basis of antimicrobial actions of silver nanoparticles. Front Microbiol 7:1831. https://doi.org/10.3389/fmicb.2016.01831

Fuerst PA, Booton GC, Crary M (2015) Phylogenetic analysis and the evolution of the 18S rRNA gene typing system of Acanthamoeba. J Eukaryot Microbiol 62(1):69–84. https://doi.org/10.1111/jeu.12186

Girois SB, Chapuis F, Decullier E, Revol BGP (2006) Adverse effects of antifungal therapies in invasive fungal infections: review and meta-analysis. Eur J Clin Microbiol Infect Dis 25(2):138–149. https://doi.org/10.1007/s10096-005-0080-0

Grace AN, Pandian K (2007) Antibacterial efficacy of aminoglycosidic antibiotics protected gold nanoparticles—a brief study. Colloid Surf A: Physicochem Eng ASp 297(1-3):63–70. https://doi.org/10.1016/j.colsurfa.2006.10.024

Ishibashi Y, Matsumoto Y, Kabata T, Watanabe R, Hommura S, Yasuraoka K, Ishii K (1990) Oral itraconazole and topical miconazole with débridement for *Acanthamoeba* keratitis. Am J Ophtalmol 109(2):121–126. https://doi.org/10.1016/S0002-9394(14)75974-4

Khan NA (2006) *Acanthamoeba*: biology and increasing importance in human health. FEMS Microbiol Rev 30(4):564–595. https://doi.org/10.1111/j.1574-6976.2006.00023.x

Khan NA, Siddiqui R (2009) *Acanthamoeba* affects the integrity of human brain microvascular endothelial cells and degrades the tight junction proteins. Int J Parasitol 39(14):1611–1616. https://doi.org/10.1016/j.ijpara.2009.06.004

Li X, Robinson SM, Gupta A, Saha K, Jiang Z, Moyano DF, Sahar A, Riley MA, Rotello VM (2014) Functional gold nanoparticles as potent antimicrobial agents against multi-drug-resistant bacteria. ACS Nano 8(10):10682–10686. https://doi.org/10.1021/nn5042625

Maincent P, Le Verge R, Sado P, Couvreur P, Devissaguet JP (1986) Disposition kinetics and oral bioavailability of vincamine-loaded polyalkyl cyanoacrylate nanoparticles. J Pharm Sci 75(10):955–958. https://doi.org/10.1002/jps.2600751009

Marciano-Cabral F, Cabral G (2003) *Acanthamoeba* spp. as agents of disease in humans. Clin Microbiol Rev 16(2):273–307. https://doi.org/10.1128/CMR.16.2.273-307.2003

Martinez AJ, Visvesvara GS (1991) Laboratory diagnosis of pathogenic free-living amoebas: *Naegleria*, *Acanthamoeba*, and *Leptomyxid*. Clin Lab Med 11(4):861–872

Martín-Navarro CM, López-Arencibia A, Sifaoui I, Reyes-Batlle M, Valladares B, Martínez-Carretero E, Piñero JE, Maciver SK, Lorenzo-Morales J (2015) Statins and voriconazole induce programmed cell death in *Acanthamoeba castellanii*. Antimicrob

Agents Chemother 59(5):2817–2824. https://doi.org/10.1128/AAC.00066-15

O'Connell KM, Hodgkinson JT, Sore HF, Welch M, Salmond GP, Spring DR (2013) Combating multidrug-resistant bacteria: current strategies for the discovery of novel antibacterials. Angew Chem Int Ed 52(41):10706–10733. https://doi.org/10.1002/anie.201209979

Radwan MA, AlQuadeib BT, Šiller L, Wright MC, Horrocks B (2017) Oral administration of amphotericin B nanoparticles: antifungal activity, bioavailability and toxicity in rats. Drug Deliv 24(1):40–50. https://doi.org/10.1080/10717544.2016.1228715

Rodino S, Butu M, Negoescu C, Caunii A, Cristina RT, Butnariu M (2014) Spectrophotometric method for quantitative determination of nystatin antifungal agent in pharmaceutical formulations. Digest J Nanomater Biostruct 9:1215–1222

Seal DV, Hay J, Kirkness CM (1995) Chlorhexidine or polyhexamethylene biguanide for *Acanthamoeba* keratitis. Lancet 345(8942):136. https://doi.org/10.1016/S0140-6736(95)90106-X

Singh A, Sharma PK, Majumdar DK (2011) Development and validation of different UV-spectropjotometric methods for the estimation of fluconazole in bulk and in solid dosage form. Indian J Chem Technol 18:357–362

Sissons J, Alsam S, Stins M, Rivas AO, Morales JL, Faull J, Khan NA (2006) Use of in vitro assays to determine effects of human serum on biological characteristics of *Acanthamoeba castellanii*. J Clin Microbiol 44(7):2595–2600. https://doi.org/10.1128/JCM.00144-06

Thomson S, Rice CA, Zhang T, Edrada-Ebel R, Henriquez FL, Roberts CW (2017) Characterisation of sterol biosynthesis and validation of 14α-demethylase as a drug target in *Acanthamoeba*. Sci Rep 7(1):8247. https://doi.org/10.1038/s41598-017-07495-z

Visvesvara GS, Moura H, Schuster FL (2007) Pathogenic and opportunistic free-living amoebae: *Acanthamoeba* spp., *Balamuthia mandrillaris*, *Naegleria fowleri*, and *Sappinia diploidea*. FEMS Immunol Med Microbiol 50(1):1–26. https://doi.org/10.1111/j.1574-695X.2007.00232.x

Walsh MD, Hanna SK, Sen J, Rawal S, Cabral CB, Yurkovetskiy AV, Fram RJ, Lowinger TB, Zamboni WC (2012) Pharmacokinetics and antitumor efficacy of XMT-1001, a novel, polymeric topoisomerase I inhibitor, in mice bearing HT-29 human colon carcinoma xenografts. Clin Cancer Res 18(9):2591–2602. https://doi.org/10.1158/1078-0432.CCR-11-1554

Wilczewska AZ, Niemirowicz K, Markiewicz KH, Car H (2012) Nanoparticles as drug delivery systems. Pharmacol Rep 64(5):1020–1037. https://doi.org/10.1016/S1734-1140(12)70901-5

Yang X, Yang J, Wang L, Ran B, Jia Y, Zhang L, Yang G, Shao H, Jiang X (2017) Pharmaceutical intermediate modified gold nanoparticles: against multidrug-resistant bacteria and wound-healing application via electrospun ccaffold. ACS Nano 11(6):5737–5745. https://doi.org/10.1021/acsnano.7b01240

Zazo H, Colino CI, Lanao JM (2016) Current applications of nanoparticles in infectious diseases. J Control Release 224:86–102. https://doi.org/10.1016/j.jconrel.2016.01.008

Zhao G, Stevens SE (1998) Multiple parameters for the comprehensive evaluation of the susceptibility of *Escherichia coli* to the silver ion. Biometals 11(1):27–32. https://doi.org/10.1023/A:1009253223055